DTIC FILE COPY

SECU

NTATION PAGE

Form Approved
OMB No. 0704-0188

1a. R
L

AD-A223 007

1b. RESTRICTIVE MARKINGS

2a. SI

3. DISTRIBUTION/AVAILABILITY OF REPORT
Approved for public release; distribution unlimited.

2b. DECLASSIFICATION/DOWNGR SCHEDULE

4. PERFORMING ORGANIZATION REPORT NUMBER(S)
Technical Report #2

5. MONITORING ORGANIZATION REPORT NUMBER(S)

6a. NAME OF PERFORMING ORGANIZATION
Dalhousie University
Physics Department

6b. OFFICE SYMBOL (If applicable)

7a. NAME OF MONITORING ORGANIZATION
Dept. of the Navy, ONR, Res. Rep.
Ohio State University Research Ctr.

6c. ADDRESS (City, State, and ZIP Code)
Halifax, Nova Scotia, Canada
B3H 3J5

7b. ADDRESS (City, State, and ZIP Code)
1314 Kinnear Rd. Room 318
Columbus, OH 43212-1194

8a. NAME OF FUNDING/SPONSORING ORGANIZATION
Office of Naval Research

8b. OFFICE SYMBOL (If applicable)

9. PROCUREMENT INSTRUMENT IDENTIFICATION NUMBER
N00014-80-J-1796

8c. ADDRESS (City, State, and ZIP Code)
800 N. Quincy St.
Arlington, VA 22217-5000

10 SOURCE OF FUNDING NUMBERS

PROGRAM ELEMENT NO	PROJECT NO	TASK NO	WORK UNIT ACCESSION NO

11. TITLE (Include Security Classification)
"Field-induced Surface Chemistry of NO"

12 PERSONAL AUTHOR(S)
H.J. Kreuzer and L.C. Wang

13a. TYPE OF REPORT	13b. TIME COVERED	14. DATE OF REPORT (Year, Month, Day)	15 PAGE COUNT
Interim Technical Report	FROM Feb.90 TO June'90	May 25, 1990	18

16 SUPPLEMENTARY NOTATION
Accepted for publication in the Journal of Chemical Physics

17 COSATI CODES		
FIELD	GROUP	SUB-GROUP

18 SUBJECT TERMS (Continue on reverse if necessary and identify by block number)
Field-induced chemistry, theory of adsorption, field-induced dissociation

19 ABSTRACT (Continue on reverse if necessary and identify by block number)

A microscopic theory of field adsorption is used to study the adsorption and reaction of NO on a Pt(111) surface in high electrostatic fields. We find that below 0.4V/Å only NO is stably adsorbed. Above this value dissociation sets in that leads around 1.2V/Å to the formation of N_2O. A molecular orbital analysis is advanced to show the reaction pathway and to identify the stabilization mechanism.

20 DISTRIBUTION/AVAILABILITY OF ABSTRACT
☒ UNCLASSIFIED/UNLIMITED ☐ SAME AS RPT ☐ DTIC USERS

21 ABSTRACT SECURITY CLASSIFICATION
Unclassified

22a NAME OF RESPONSIBLE INDIVIDUAL	22b TELEPHONE (Include Area Code)	22c OFFICE SYMBOL
H.J. Kreuzer	(902) 494-6594	

DD Form 1473, JUN 86 Previous editions are obsolete SECURITY CLASSIFICATION OF THIS PAGE

S/N 0102-LF-014-6603

OFFICE OF NAVAL RESEARCH

GRANT: N00014-80-J-1796

R&T Code 4131054 - 2

Technical Report No. 2

Field-induced Surface Chemistry of NO

by

H.J. Kreuzer and L.C. Wang

Submitted for Publication

to

Journal of Chemical Physics

Dalhousie University
Department of Physics
Halifax, Nova Scotia B3H 3J5

May 25, 1990

Field-induced Surface Chemistry of NO

H.J. Kreuzer and L.C. Wang

Department of Physics, Dalhousie University,

Halifax, N.S. B3H 3J5, Canada

Abstract

A microscopic theory of field adsorption is used to study the adsorption and reaction of NO on a Pt(111) surface in high electrostatic fields. We find that below 0.4V/Å only NO is stably adsorbed. Above this value dissociation sets in that leads around 1.2V/Å to the formation of N_2O. A molecular orbital analysis is advanced to show the reaction pathway and to identify the stabilization mechanism.

1. Introduction

Electric fields of the order of volts per angstrom are comparable to those experienced by valence electrons in atoms and molecules. One should therefore expect that in external fields of that magnitude a redistribution of the valence electrons in molecules and in particular in molecules adsorbed on surfaces takes place effecting both internal bonds as well as the surface bond. Whether this redistribution leads to enhanced or reduced binding depends on whether bonding or antibonding orbitals are more strongly effected. We will refer to this phenomenon as field-induced chemistry; the physics and chemistry in high electrostatic fields has been reviewed recently [1]. To estimate the field strength needed to effect the chemistry of a reaction, we note that the equilibrium constant, K, of a reactive system depends on the field strength, F, via a van't Hoff equation [2]

$$\frac{\partial \ell nK}{\partial F} = \frac{\Delta M}{RT} \tag{1}$$

where ΔM is a partial molar energy related to the change in electric moment in the reaction, i.e.

$$\Delta M = \Delta p F + \tfrac{1}{2}\Delta\alpha F^2 + \ldots \tag{2}$$

Here Δp is the difference in the permanent dipole moments of the products and the reactants, and $\Delta\alpha$ is the change in their polarizability. In order to achieve values for ΔM comparable with typical reaction enthalpies or volumes, one needs fields in excess of $0.1 V/\mathring{A}$.

Block and coworkers have developed a field pulse technique in the field ion microscope that allows the investigation of the field effect on chemical reactions; a

detailed account has been given by Block [3]. Systems that have been studied by this technique are the formation of metal subcarbonyls, the polymerization of acetone, the reaction of sulphur on metal surfaces, the decomposition of methanol on metal surfaces, hydride formation on semiconductors, NO reactions on metals and many more.

A microscopic theory can elucidate the changes in reaction pathways induced by high electric fields. As a precursor to such field-induced chemistry, we have looked at the effect of electric fields on the vibrational frequency of a molecule adsorbed on a metal, in particular, N_2 on Fe(111) [4]. We have also studied the formation of Ru subcarbonyls as a function of field strength, being able to reproduce the essential features of the experimental data and also to suggest the geometries of these subcarbonyls [5].

In this paper, we will study theoretically the adsorption, dissociation and reaction of NO on a Pt surface. We briefly describe the experimental findings: although NO adsorbed on various planes of platinum does not dissociate at room temperature, applying steady electric fields in excess of $0.4V/\mathring{A}$ causes rapid decomposition. Employing pulsed field desorption mass spectrometry, Kruse et al [6] observed N_2O^+, N_2^+ and, to a lesser extend, O^+ ions from the stepped Pt(111) regions of a field emitter tip as the field is increased, with decreasing amounts of NO^+ being recorded. Beyond $1.2V/\mathring{A}$ no NO^+ could be desorbed anymore.

In the next section we briefly review the computational method. We represent the metal surface by a cluster of metal atoms and use the ASED-MO method to calculate the potential energy surface and possible reaction pathways of NO on platinum. We present results in section 3 starting with a study of NO adsorption on platinum in zero field. We continue with the field dependence of the adsorption geometries and energetics and present a detailed molecular orbital analysis along the reaction coordinate

2. Cluster Model

To calculate the adsorption energies and equilibrium geometries of NO and its reaction products on platinum we have represented the metal by a cluster of Pt atoms. We then employ the atom-superposition and electron-delocalization molecular orbital method (ASED-MO) [7] in which one writes the total energy of metal cluster plus adsorbate as a sum of a repulsive term, that accounts for the Coulomb interaction of isolated atoms with each other, and a remainder that entails the rearrangement within the atoms in the present of each other. The latter is calculated from a hamiltonian

$$H = \sum_{i\alpha} H_{ii}^{\alpha\alpha} \, |\phi_i^{\alpha}\rangle\langle\phi_i^{\alpha}| + \sum_{ij\alpha\neq\beta} H_{ij}^{\alpha\beta} \, |\phi_i^{\alpha}\rangle\langle\phi_j^{\beta}| \tag{3}$$

where in the spirit of an extended Hückel scheme one puts the diagonal elements

$$H_{ii}^{\alpha\alpha} = -E_i^{\alpha} \tag{4}$$

equal to the negative of the ionization energy of level i on atom α, taken from experiment. The remaining off-diagonal elements are a modification of the extended Hückel formula

$$H_{ij}^{\alpha\beta} = \kappa \, (H_{ii}^{\alpha\alpha} + H_{jj}^{\beta\beta}) S_{ij}^{\alpha\beta} \exp(-\alpha R_{\alpha\beta}) \tag{5}$$

with

$$S_{ij}^{\alpha\beta} = \langle \phi_i^{\alpha} \mid \phi_j^{\beta} \rangle \tag{6}$$

being the overlap integral between the i-th atomic orbital on atom α and the j-th orbital on atom β, the latter being a distance $R_{\alpha\beta}$ away. Fitting bond strengths and lengths to first row diatomics, one determines the parameters in (4) to be $\kappa = 1.125$ and $\alpha = 0.13\ \mathring{A}^{-1}$.

To include electric field effects [8,9] within the framework of the ASED-MO cluster calculations, we note that in the notation of (3) we have to add terms

$$H_{ij}^{\alpha\beta(F)} = \int \phi_i^{\alpha}(\mathbf{r})^* V_F(\mathbf{r}) \phi_j^{\beta}(\mathbf{r}) d\mathbf{r} \tag{7}$$

where the field potential is given by

$$V_F(\mathbf{r}) = e \int_{-\infty}^{\mathbf{r}} \mathbf{F}(\mathbf{r}') \cdot d\mathbf{r}' \tag{8}$$

Additionally one must, of course, also add the field energy of the nuclei

$$- \sum_{\alpha} Z_{\alpha} V_F(R_{\alpha}) \tag{9}$$

where Z_{α} is the charge of the α-th nucleus.

In (8) we write

$$V_F(\mathbf{r}) = V_F(R_\alpha) + V_F(\mathbf{r}) - V_F(R_\alpha) \tag{10}$$

and get

$$H_{ij}^{\alpha\beta(F)} = V_F(R_\alpha)\, S_{ij}^{\alpha\beta} + \int \phi_i^{\alpha}(\mathbf{r})^*[V_F(\mathbf{r}) - V_F(R_\alpha)]\phi_j^{\beta}(\mathbf{r})d\mathbf{r} \tag{11}$$

which we approximate, for an electric field in the z direction depending on z only, by

$$H_{ij}^{\alpha\beta(F)} = \tfrac{1}{2}[V_F(R_\alpha)+V_F(R_\beta)+\langle\psi_i^{\alpha}|(V_F(z)-V_F(z_\alpha)|\psi_i^{\alpha}\rangle+\langle\psi_j^{\beta}|(V_F(z)-V_F(z_\beta)|\psi_j^{\beta}\rangle]\, S_{ij}^{\alpha\beta} \tag{12}$$

The diagonal parts of the first two terms in (12) lead to the raising of the energy levels in (4) by the field energy as done in our previous work, i.e.,

$$H_{ii}^{\alpha\alpha} = (E_i^{\alpha} + V_F(R_\alpha)) \tag{13}$$

The off-diagonal parts of the first two term in (12) are obviously proportional to the overlap integrals between atomic orbitals on different atoms and are accounted for by modifying the Hückel-type hopping matrix elements (5) by again raising the energy levels by the field energy. This approximation seems to be the most natural in the context of an extended Hückel model. Note that the second term in (11) for $\alpha \neq \beta$ is expressed in (12) in terms of matrix elements on the same atom.

To evaluate the third term in (12), we note that over the extent of the atom α the electric field varies little. We can therefore employ a Taylor expansion to get

$$V_F(z) - V_F(z_\alpha) = (z-z_\alpha)eF(z_\alpha) + \tfrac{1}{2}(z-z_\alpha)^2 eF'(z_\alpha) + \ldots \quad (14)$$

A proper theory of field effects on surfaces must include a selfconsistent determination of the externally applied electric field in the vicinity within a few angstroms of either side of the metal surface. Model calculations have recently become available that use functional density methods to calculate the local electric field and the excess surface charge at the surface of a metal, treating the latter as a structureless jellium of uniform positive charge (rather than a lattice of positive ions) to which an electron gas reacts within the local density approximation[10,11]. Earlier work in this field is reviewed in these references. The important points to note are that the center of mass z_0 of the induced charge density, i.e., the effective image plane of a charge situated outside the jellium, lies half to one angstrom outside the jellium edge, decreasing with increasing surface charge, i.e., applied electric field. We recall that the jellium edge is typically put half an interplanar distance outside the topmost lattice plane. It is also noteworthy that, although the electric field has reached its asymptotic value some 2Å above the surface where adsorption typically takes place, the associated energy is only a fraction of its value, had we approximated the field as being constant all the way to the position of the top metal atom. On the other hand, taking the field constant up to the image plane z_0, identified as the center of mass of the field-induced surface charge, yields a very good approximation to the field energy a few angstroms above the surface.

We stress that these model calculations are for a flat, structureless metal (jellium) surface. The major additional complication in the case of field effects on real surfaces arises from the fact that electric fields are greatly enhanced at adsorption sites, namely at kink sites, at terraces and around small atom clusters

on top of extended planes. Such inhomogeneities are extremely difficult to calculate reliably. All we can do at the present stage is to incorporate some of the insight gained in the above jellium calculations into our cluster calculations in an ad hoc way. This procedure has been applied successfully to field adsorption [8,12], field desorption [13,14] and field evaporation [9]. However, this should not negate the need to eventually perform a calculation in which the electronic degrees of freedom, the lattice structure and local field effects are treated in a selfconsistent way.

The parameters used in our numerical work, i.e. ionization energies and Slater exponents, are listed in Table 1. To take over the electric field variation in front of the metal from jellium calculations, we assign a value r_s=2.0 to platinum.

3. NO Adsorption on Pt(111)

XPS, EELS and IRS experiments have provided evidence that NO adsorbs on Pt(111) [15] (and on Ni(111) [16] and Ru(001) [17]) in bridge sites at low coverage and in on-top sites at higher coverages with about the same binding energies. In particular on Pt(111) the bridge-bonded NO has a dipole moment of 0.42D with the negative O end outward in accordance with multiply-coordinated NO groups in large molecules, whereas the linearly bonded on-top species has a positive dipole moment with the O end positively charged as it happens with terminal NO groups. This flexibility is due to the lonely electron in the 2π antibonding level, consisting mainly of the $2p_x$ levels of O and N. This picture has been confirmed by our ASED-MO calculations as demonstrated in panel A of Fig.1 where we plot the electron density contours of adsorbed NO in zero field.

As an electric field is applied, the levels on the O atom, being further away from the surface, are raised up relatively higher than those on the N atom. This in

particular effects the $2p_x$ levels on O and N resulting in a shift of the electronic charge of the 2π level to the O atom, as illustrated in panel B of Fig.1. As a result the overlap between the 2π level of NO and the levels of the metal decreases with a subsequent decrease in the electron transfer from the metal to the 2π level stabilizing the adsorbed NO molecule. Also note that the dipole moment of adsorbed NO, i.e. O^-N^+, is opposite to the field direction, thus the total energy increases as the field is increased.

Looking next at the bending mode of adsorbed NO, we note that as the molecular axis of NO bends away from the surface normal, the O atom moves into regions where the electric field energy is less, e.g. in the extreme case where the NO axis is parallel to the surface, N and O would experience the same field. Thus bending away from the surface normal reduces the electric field effect, i.e. the electronic distribution of the 2π level moves closer to the metal leading to an increase in the charge transfer from the metal, as illustrated in panels C and D of Fig.1. This trend is summarized in Fig.2 where we plot the charge transfer from the metal into the 2π level as a function of the angle from the surface normal for various field strengths. With the electron distribution of the 2π level shifting back from the O atom to the N atom as bending takes place away from the surface normal, the additional charge in the 2π level leads eventually to the decomposition of the adsorbed NO molecule. Energies and geometries are depicted in Fig.3 as a function of the reaction coordinate, indicating the dramatic decrease in the activation barrier for dissociation as a function of field strength due to the dipole moment of adsorbed NO being along the vibrational direction. We should point out that the ASED-MO method is not very reliable in its predictions of absolute energies; however, the trends as a function of reaction coordinates and field strength should be trustworthy.

4. NO Reaction

We next look at a situation where, in a field larger than about 0.4V/Å a NO molecule is adsorbed next to a N atom, the latter the result of dissociation. As depicted in Fig.4 the bending vibrations of the two species towards each other can result in such close approaches that a strong N-N bond can establish itself. For fields larger than 1.2V/Å the reduction of the activation barrier becomes so significant that the NO molecule will snap on top of the adsorbed N atom leading to the formation of adsorbed N_2O.

To understand the mechanism of N_2O formation, we look in detail at the participating molecular orbitals. First we note that the electron transfer between the adsorbed N_2O and the metal mainly involves the 6σ, 7σ abd 2π orbitals of N_2O. The 6σ level is antibonding consisting mainly of O $2p_z$, mixed with O 2s, and the antibonding level of N_2 originating from the 2s levels. In zero field the charge in the 6σ level is mainly on the O atom. Next, the 7σ level is bonding, resulting from the combination of the O $2p_z$ level and the bonding level of N_2, namely 5σ resulting from the combination of the $2p_z$ levels of the two N atoms. In zero field the charge is centered on the first N atom, i.e. the one closest to the metal. Lastly, the 2π level is nonbonding. In our calculation we found that in zero field the N_2O molecule will decompose upon adsorption into an adsorbed N_2 and most likely a free O.

As we increase the electric field, the electronic configuration of adsorbed N_2O changes drastically. Looking first at the 6σ level, Fig.5, we note that as the field is increased, the O $2p_z$ level is raised relative to the the 2s levels on the N atoms resulting in the center of gravity of the charge distribution in the 6σ level to shift to the N atom closest to the metal thus strengthening the bond to the metal and increasing the electron charge transferred from the antibonding 6σ level of N_2O to the metal, leading to the stabilization of the adsorbed N_2O. As for the 7σ level,

Fig.6, the decreased energy difference between the C $2p_z$ and the $2p_z$ level on the N farthest from the metal and the increased energy difference between the $2p_z$ levels on the two N atoms, results in a shift of the electronic charge to the O atom thus decreasing the overall charge transfer from the 7σ level to the metal. In terms of dipole moments, the situation in low field is metal-N^-N^+-O^- whereas in fields in excess of $0.8V/\mathring{A}$ we have metal-N^--N^+-O^+. Thus the chemical structure of adsorbed N_2O is stabilized in fields of this magnitude.

We can shed more light on the stabilisation of N_2O in a field by looking at the bending vibrations. As we saw earlier, bending an adsorbed molecule away from the normal brings it closer to equipotential surfaces, thus reducing the field effect. In particular for N_2O, the center of charge on the 6σ level shifts back to the O atom reducing the charge transfer to the metal, panels C and D of Fig.5. As for the 7σ level, its charge distribution shifts back to the N atom closest to the metal increasing the charge transferred to the metal, panels C and D of Fig.6. The charge transfer from the 6σ and 7σ levels are given as a function of bending angle in Fig.7. In closing we note that the force constant of the vibrational potential gets larger as the field increases, cf. Fig.4.

5. Summary

In this paper we have presented an analysis of the adsorption and reaction characteristics of NO on a Pt(111) surface. We have been able to explain the field dependence of NO dissociation and N_2O formation obtaining very good agreement with the reaction field strengths measured [6]. Furthermore, a detailed molecular orbital analysis identifies the underlying reaction mechanisms. Although the overall picture is consistent with experimental data, we should be aware of the fact that the theory is rather crude at this stage in that we use the semi-empirical ASED-MO method rather than some ab initio procedure. We hope to pursue the latter route in the

near future.

This investigation has been initiated by experiments in the field ion microscope. We would, however, point out that field-induced chemistry also takes place at the electrode-electrolyte interface and in the vicinity of charge impurities on catalysts. Unfortunately, little is known about local field strengths in these systems; still, our theoretical results should have at least qualitative implications for catalysis and electrochemistry.

Acknowledgment

This work was supported in part by a CRD grant from NSERC and CIL, and the Office of Naval Research.

References

[1] H.J. Kreuzer, in Physics and Chemistry at Solid Surfaces VIII, ed. R. Vanselow (Springer-Verlag, Berlin, 1990).

[2] K. Bergmann, M. Eigen and L. de Maeyer, Ber. Bunsenges. Phys. Chem. 67 (1963) 819.

[3] J.H. Block, in Physics and Chemistry at Solid Surfaces IV, eds. R. Vanselow and R. Howe (Springer-Verlag, Berlin, 1982).

[4] D. Tomanek, H.J. Kreuzer, and J.H. Block, Surf. Sci. 157, L315 (1984).

[5] L.C. Wang and H.J. Kreuzer, J. de Physique 50 C-8 (1989) 53.

[6] N. Kruse, G. Abend and J.H. Block, J. Chem. Phys. 88(1988) 1307.

[7] A.B. Anderson and R.G. Parr, J. Chem. Phys. 53, 3375 (1969); A.B. Anderson, J. Chem. Phys. 60, 2477 (1973), 62, 1187 (1974), 63, 4430 (1974).

[8] K. Nath, H.J. Kreuzer, and Alfred B. Anderson, Surf. Sci. 176 (1986) 261.

[9] H.J. Kreuzer and K. Nath, Surf. Sci. 183 (1987) 591.

[10] P. Gies and R.R. Gerhardts, Phys. Rev. B 31, 6843 (1985); 33, 982 (1986).

[11] F. Schreier and F. Rebentrost, J. Phys. C:Solid State Phys. 20 (1987) 2609.

[12] N. Ernst, W. Drachsel, Y. Lin, J.H. Block, and H.J. Kreuzer, Phys. Rev. Lett. 57, 2686 (1986).

[13] H.J. Kreuzer and L.C. Wang, J. de Physique 50 C-8 (1989) 9.

[14] H.J. Kreuzer, L.C. Wang and K. Watanabe, Surf. Sci. (in press).

[15] M. Kiskinova, G. Pirug, and H.P. Bonzel, Surface Sci. 136 (1984) 285.

[16] M.J. Breitschafter, E. Umbach, and D. Menzel, Surface Sci. 109 (1981) 493.

[17] P. Feulner, S. Kulkarni, E. Umbach, and D. Menzel, Surface Sci. 99 (1980) 489.

Table 1: Ionization energies E_I and Slater exponents ζ for the atomic orbitals used. The d-orbitals contain terms $C_1\exp(-\zeta r)+C_2\exp(-\zeta' r)$. Also given are the initial occupation of the various orbitals.

		E_I(eV)	ζ(Å^{-1})	ζ'(Å^{-1})	C_1	C_2	in.occ.
N	2s	19.13	1.924				2
	2p	12.14	1.917				3
O	2s	27.28	2.146				2
	2p	13.62	2.127				4
Pt	6s	10.20	2.550				2
	6p	6.16	2.250				0
	5d	10.8	6.013	2.39	0.6567	0.5715	8

Figure captions

Fig.1: Charge density contours, ρ, of 2π orbital around adsorbed NO with N open circle and O full dot. Contour lines are ±0.005, ±0.01, ±0.02, ±0.04, 0.06, 0.12 electron/$\mathring{A}^3$. Panels A and C: ρ in zero field; panels B and D: $\rho(F=1.2V/\mathring{A})$ - $\rho(F=0)$.

Fig.2: Charge transfer into the 2π orbital of NO.

Fig.3: Potential energy curves and adsorption geometries of NO on Pt(111) as a function of reaction coordinate.

Fig.4: Potential energy curves and adsorption geometries of NO+N on Pt(111) as a function of reaction coordinate.

Fig.5: Charge density contours, ρ, of 6σ orbital around adsorbed N_2O with N open circle and O full dot. Contour lines are ±0.005, ±0.01, ±0.02, ±0.04, 0.08, 0.16 electron/$\mathring{A}^3$. Panels A and C: $\rho(F=0.4V/\mathring{A})$; panels B and D: $\rho(F=0.8V/\mathring{A})$ - $\rho(F=0.4V/\mathring{A})$.

Fig.6: Charge density contours, ρ, of 7σ orbital around adsorbed N_2O with N open circle and O full dot. Contour lines are ±0.005, ±0.01, ±0.02, ±0.04, 0.08, 0.16 electron/$\mathring{A}^3$. Panels A and C: $\rho(F=0.4V/\mathring{A})$; panels B and D: $\rho(F=0.8V/\mathring{A})$ - $\rho(F=0.4V/\mathring{A})$.

Fig.7: Charge transfer from the 6σ and 7σ orbitals of N_2O.

Fig. 1

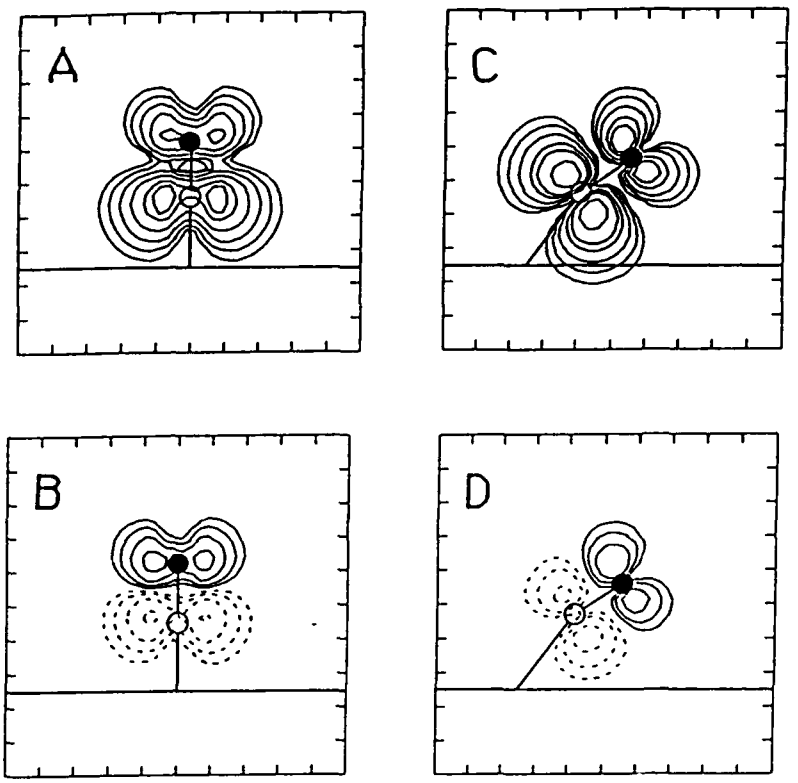
A
C
B
D

Fig. 2

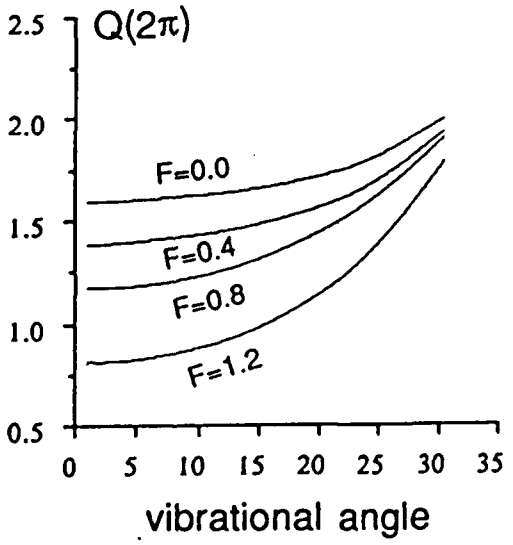
Q(2π)
2.5
2.0
1.5
1.0
0.5
F=0.0
F=0.4
F=0.8
F=1.2
0
5
10
15
20
25
30
35
vibrational angle

Fig. 3

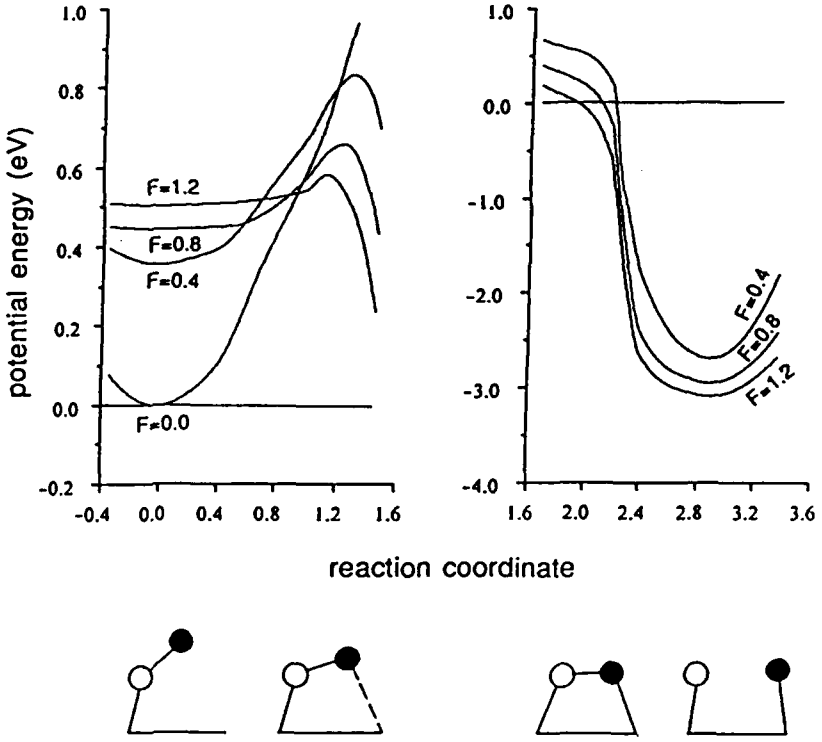
potential energy (eV)
reaction coordinate
F=1.2
F=0.8
F=0.4
F=0.0
F=0.4
F=0.8
F=1.2

Fig. 4

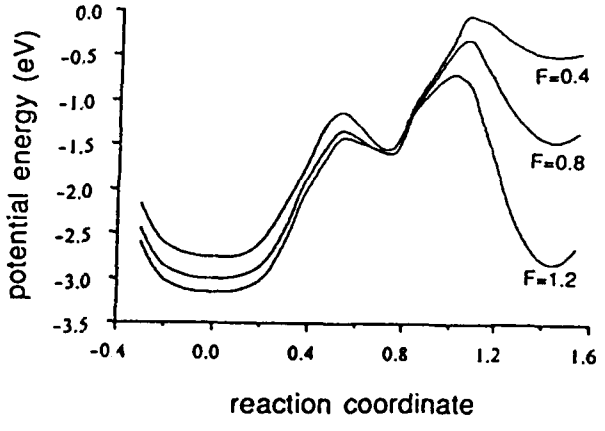
potential energy (eV)
reaction coordinate
F=0.4
F=0.8
F=1.2

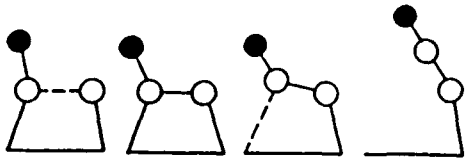

Fig. 5

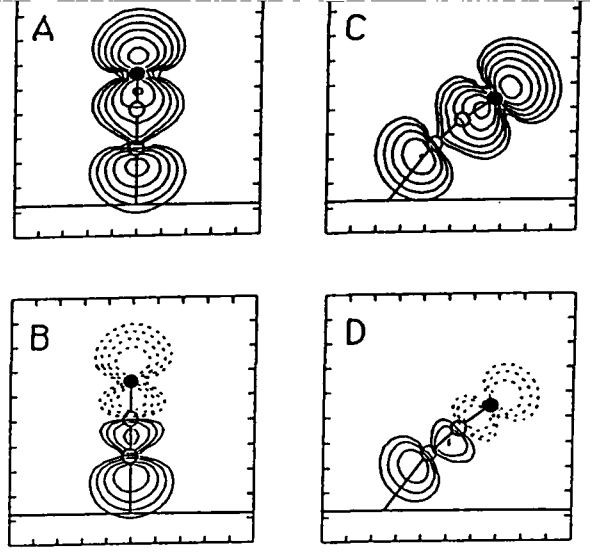

Fig. 6

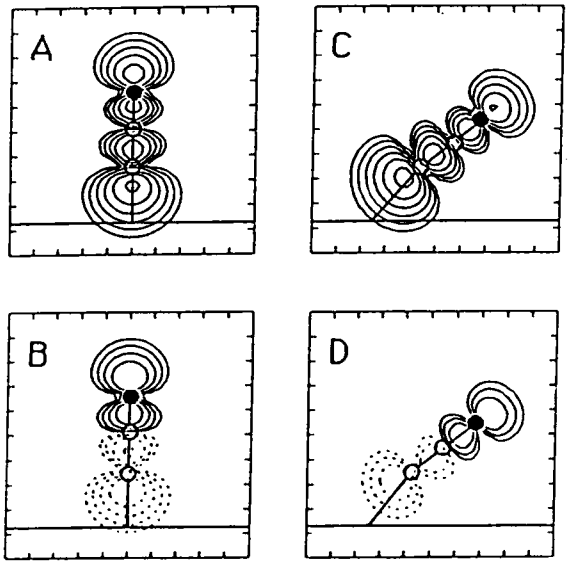

Fig. 7